Hyperfine Interact (2018) 239:5
https://doi.org/10.1007/s10751-017-1479-6

Spleen tissues from patients with lymphoma: magnetization measurements and Mössbauer spectroscopy

I. V. Alenkina[1] · A. V. Vinogradov[2,3] · T. S. Konstantinova[3] · I. Felner[4] · M. I. Oshtrakh[1]

Abstract Spleen tissues from five patients with two types of non-Hodgkin B-cells lymphomas, namely, mantle cell lymphoma and marginal zone B-cell lymphoma, and one sample of healthy human spleen tissue were studied using Mössbauer spectroscopy and magnetization measurements. Magnetization measurements demonstrated small differences in the saturation magnetic moments and the presence of paramagnetic components. Mössbauer spectra of spleen tissues demonstrated some variations in the relative content of ferritin-like iron in tissues as well as small variation in the hyperfine parameters for normal and patients' spleen tissues. Some changes in the ferritin iron core structure in patients' spleen were suggested in comparison with normal subject.

Keywords Mössbauer spectroscopy · Magnetization measurements · Ferritin-like iron · Spleen Tissue · Non-Hodgkin B-cells lymphoma

This article is part of the Topical Collection on *Proceedings of the International Conference on the Applications of the Mössbauer Effect (ICAME 2017), Saint-Petersburg, Russia, 3–8 September 2017*
Edited by Valentin Semenov

✉ M. I. Oshtrakh
oshtrakh@gmail.com

[1] Department of Experimental Physics, Institute of Physics and Technology, Ural Federal University, Ekaterinburg, 620002, Russian Federation

[2] Sverdlovsk Regional Ministry of Health, Weiner str., 34b, Ekaterinburg, 620014, Russian Federation

[3] Sverdlovsk Regional Clinical Hospital No 1, Volgogradskaya str., 185, Ekaterinburg, 620102, Russian Federation

[4] Racah Institute of Physics, The Hebrew University, Jerusalem, 91904 Israel

Published online: 13 December 2017

1 Introduction

Mammalian spleen tissues contain a large amount of iron. This is related to a very important role of spleen in the body because spleen is an organ for utilization of red blood cells and hemoglobin. An iron released after hemoglobin utilization is toxic but still needed for further synthesis of iron containing proteins. To avoid toxic effect of free iron and provide its bioavailability, spleen cells synthesize the protein apoferritin which can accumulate iron ions and keep it in the non-toxic form available for organism's needs. This iron storage protein ferritin consists of a protein shell and nano-sized ferric hydrous oxide core [1]. Ferritin iron core has a complex structure and in spite of a long time of its investigation there is no exact information about its structure. Several iron core models, reflecting some peculiarities of the core and the methods of investigation, were developed and considered, for instance, in [2–6].

Mössbauer spectroscopy is a powerful tool to study iron storage proteins even in tissues (see for review [7–9]). Further development of technique and application of Mössbauer spectroscopy with a higher order of discretization of the velocity reference signal (so called Mössbauer spectroscopy with a high velocity resolution) permitted us to increase precision and accuracy of spectra measurement and further raise the analytical possibilities of technique. Some advances of this method have been recently considered in [10, 11] as well as biomedical application was described in [12–14]. It is well known that some diseases are accompanied by the iron status disorders. Therefore, Mössbauer spectroscopy could be useful in order to investigate spleen tissues from various patients. We have started a study of spleen and liver tissues from patients with hematological malignancies and observed some changes in the iron content and in the ^{57}Fe hyperfine parameters of ferritin-like iron in patients' tissues [15, 16, 18]. Owing to the problem to get fresh patient's tissues we have studied in [17, 18] spleen from three patients only with different hematological malignancies. Now we consider the results for spleen tissues obtained from five patients with lymphoma. Magnetization measurements are also a useful technique to study ferritin [7]. For instance, on the basis of observation of the paramagnetic component in the isothermal magnetization curve the iron core-shell model was developed [2]. Therefore, we use both techniques to study spleen tissues from some patients with lymphomas.

2 Experimental

Spleen tissues from patients with two cases of non-Hodgkin B-cells lymphomas such as mantle cell lymphoma (MCL) and marginal zone B-cell lymphoma (MZL) were studied. Spleen tissues were obtained at the Hematological Division of the Sverdlovsk Regional Clinical Hospital No 1 (Ekaterinburg, Russian Federation) under all human rights and ethical guidelines from two patients with MCL (MCL 1 and MCL 2) and three patients with MZL (MZL 1, MZL 2 and MZL 3). One sample of healthy human spleen tissue (NOR) was used for comparison. All spleen samples were taken after splenectomy except MZL 1 which was taken post mortem. Then diagnoses were confirmed by histological and immunohistochemical analyzes. Spleen tissues were washed from blood, lyophilized and powdered for further study using DC magnetization measurements and Mössbauer spectroscopy. For Mössbauer studies, sample powders with weights of 900 mg (NOR), 1335 mg (MCL 1), 1400 mg (MCL 2), 938 mg (MZL 1), 1530 mg (MZL 2) and 700 mg (MZL 3) were packed into the Plexiglas sample holders with a diameter of 20 mm and height in the range 10–15 mm depending on the sample volume.

Mössbauer spectra of all samples were measured using an automated precision Mössbauer spectrometric system built on the base of the SM-2201 spectrometer with a high velocity resolution at the Institute of Physics and Technology, Ural Federal University (Ekaterinburg, Russian Federation). This spectrometer operates with a saw-tooth shape velocity reference signal formed by the digital-analog converter using discretization of 2^{12} (quantification using 4096 steps). Details and characteristics of this spectrometer and the system were given elsewhere [10, 11, 19, 20]. The $\sim 1.8 \times 10^9$ Bq ^{57}Co in rhodium matrix source (Ritverc GmbH, St. Petersburg) was used at room temperature (RT). Mössbauer spectra were measured in transmission geometry with moving absorber at 295 K and recorded in 4096 channels. For their analysis, these spectra were converted into 1024 channels by a consequent summation of four neighboring channels to increase signal-to-noise ratio due to poor iron content in tissues. Statistical counts in the 1024-channel normal spleen spectrum was $\sim 6.4 \times 10^6$ counts per channel with a signal-to-noise ratio of 8 while that for the patients' spleen spectra were from $\sim 2.5 \times 10^6$ to $\sim 4.0 \times 10^6$ counts per channel with a signal-to-noise ratio ranged from 9 to 18. Each spectrum was measured up to 4 weeks.

The Mössbauer spectra were computer fitted with the least squares procedure using UNIVEM-MS program with a Lorentzian line shape. The spectral parameters such as isomer shift, δ, quadrupole splitting, ΔE_Q, line width, Γ, relative subspectrum area, A, and statistical criterion, χ^2, were determined. An instrumental (systematic) error for each spectrum point was ± 0.5 channel (the velocity scale), the instrumental (systematic) error for the hyperfine parameters was ± 1 channel. If an error calculated with the fitting procedure (fitting error) for these parameters exceeded the instrumental (systematic) error we used the larger error instead. The relative error for A did not exceed 10%. Criteria of the best fit were differential spectrum, χ^2 value and physical meaning of parameters. The standard absorber of sodium nitroprusside (SNP) with a thickness of 5 mg Fe/cm^2 was used for velocity scale calibration. The Mössbauer spectra of SNP demonstrated pure Lorentzian line shape with $\Gamma = 0.226 \pm 0.010$ mm/s. Velocity resolution in the 1024-channel spectra of spleen tissues was of 0.005 mm/s per channel. Values of δ are given relatively to α-Fe at 295 K.

Magnetization measurements on tissue samples (about 6–14 mg) mounted in gel-caps at various applied magnetic fields (H) in the temperature interval $5\ K < T < 300\ K$, have been performed using a Quantum Design superconducting quantum interference device (SQUID) magnetometer at the "Racah" Institute of Physics, the Hebrew University (Jerusalem, Israel). The differential SQUID sensitivity is 10^{-7} emu. Prior to recording each zero-field-cooled (ZFC) curve, the magnetometer was adjusted to be in a "real" $H = 0$ state. Then, the samples were cooled to the desired temperatures and the field was switched on to trace the various ZFC branches of the magnetization M(T) curves. Under this field, the field-cooled (FC) branches were measured via warming from low to high temperatures via heating.

3 Results and discussion

Mössbauer spectra of normal and patients' spleen tissues measured at RT are shown in Fig. 1. These spectra demonstrate two peaks shape corresponding to ferritin-like iron with admixture of a minor component related to residual methemoglobin. The ferritin-like subspectra were fitted using two quadrupole doublets within the simple heterogeneous iron core model (see [18]) as Mössbauer spectra of spleen tissues demonstrated a very small absorption effect (between ~ 0.2 and $\sim 0.4\%$) and a low signal-to-noise ratio. On the basis of the total area of ferritin-like components normalized by the sample weight, the relative ferritin-like iron content was evaluated and presented in Fig. 2. The relative ferritin-like

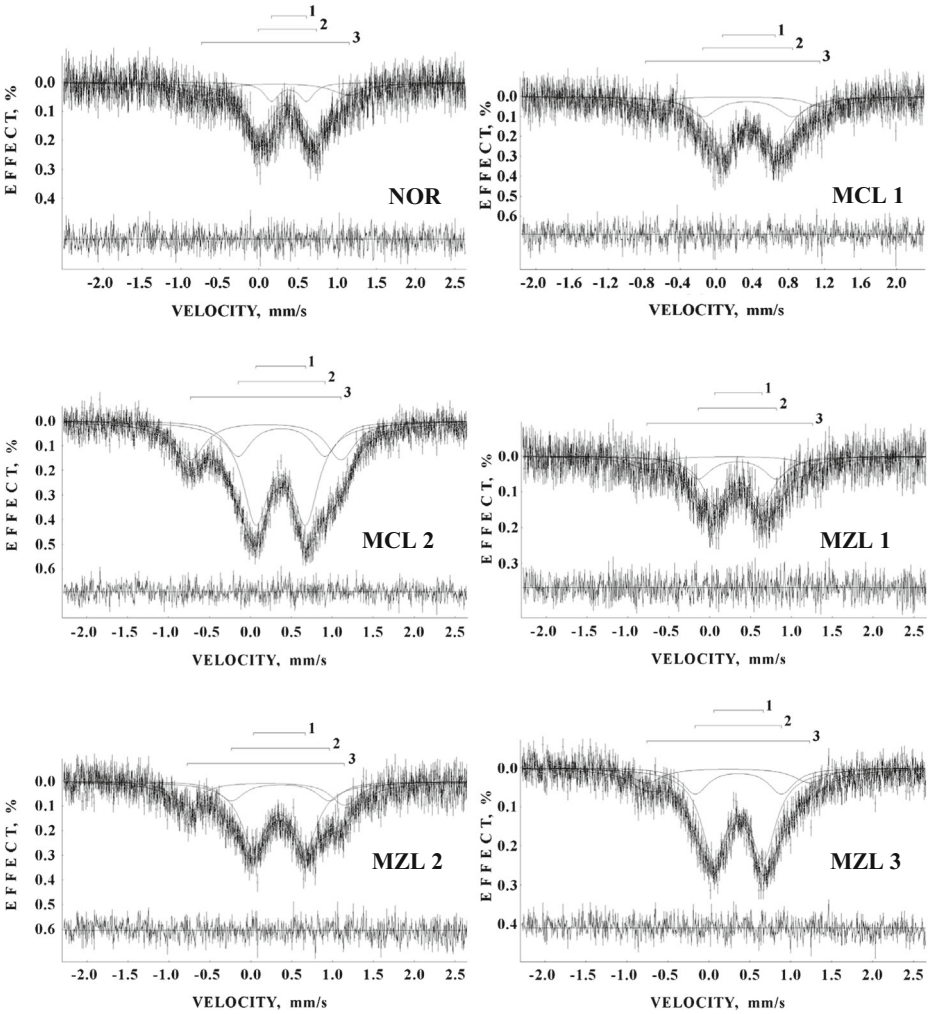

Fig. 1 Mössbauer spectra of normal human spleen (**NOR**) and spleen from patients with mantle cell lymphoma (**MCL 1** and **MCL 2**) and marginal zone B-cell lymphoma (**MZL 1**, **MZL 2** and **MZL 3**). Indicated components are the results of the best fits, components 1 and 2 are related to the ferritin-like iron core structural peculiarities while component 3 is related to residual methemoglobin. Differential spectra are shown below. T = 295 K

iron content appeared to be similar in the following spleen tissues: NOR, MZL 2 and MCL 1. On the other hand, spleen tissue MZL 1 showed a slightly smaller amount of iron than above mentioned samples while spleen tissues MZL 3 and MCL 2 demonstrated a larger amount of ferritin-like iron in comparison with other spleen tissues. These differences may be related to some individual features of patients.

The ^{57}Fe hyperfine parameters of ferritin-like components obtained from the spectra fit using the simple heterogeneous iron core model with two quadrupole doublets are shown in the plots of δ and ΔE_Q in Fig. 3. These parameters demonstrated small variations between healthy and patients' ferritin-like iron. According to the ΔE_Q values these two components

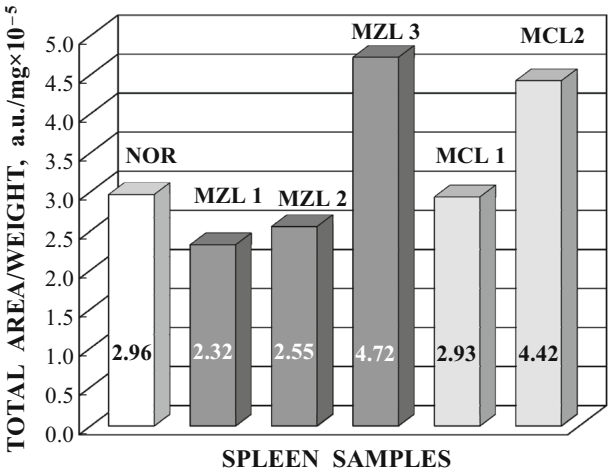

Fig. 2 Relative ferritin-like iron content in normal spleen tissue (**NOR**) and spleen tissues from patients with mantle cell lymphoma (**MCL 1** and **MCL 2**) and marginal zone B-cell lymphoma (**MZL 1**, **MZL 2** and **MZL 3**) (total area of ferritin-like spectral components normalized by the sample weight)

can be assigned to the iron core regions with different density of FeOOH packing [18, 21]. Therefore, component 1 with a smaller ΔE_Q value can be associated with more close packed FeOOH regions of the ferritin iron core while component 2 with a larger ΔE_Q value can be related to less close packed FeOOH regions. Considering this simple model [18], it is clearly seen that the δ values related to more close packed regions are similar for normal spleen tissue and spleen tissues MCL 1, MCL 2 and MZL 3 while spleen tissues MZL 1 and MZL 2 demonstrated smaller values of δ. The ΔE_Q values for more close packed FeOOH regions in the core appeared to be similar for all samples except MZL 2 with a larger value of ΔE_Q. For less close packed regions of the iron core associated with component 2, the δ values are similar for normal spleen tissue and patients' spleen tissues except MCL 2 with a larger value of δ. The ΔE_Q values of component 2 appeared to be different from that of normal spleen tissue for all patients' tissues. In this case a small increase in the ΔE_Q value may be related to a small increase in the electric field gradient on the ^{57}Fe nuclei caused by the ^{57}Fe local microenvironment distortion in the ferritin molecules from patients' spleen tissues.

Within the proposed simple heterogeneous iron core model [18] it is possible to evaluate the relative parts of more and less close packed iron core regions in ferritin molecules using the relative areas of corresponding spectral components. The results presented in Fig. 4 demonstrate differences in the relative parts of more and less close packed iron core regions with larger part of the former for all samples. However, the part of more close packed iron core regions in ferritin from normal spleen tissue appeared to be smaller than that in ferritin from patients' tissues and vice versa: the part of less close packed iron core regions in ferritin from normal spleen tissue appeared to be larger than that in ferritin from patients' tissues. This fact demonstrates that a slightly higher part of more closed packed iron core regions in ferritin molecules in patients' spleen tissues can be a result of some features in the iron accumulation in spleen ferritin during the studied cases of lymphomas.

Magnetic measurements have been performed on the same normal human and patients' spleen tissues as the Mössbauer measurements. Basically, the magnetic features of all six

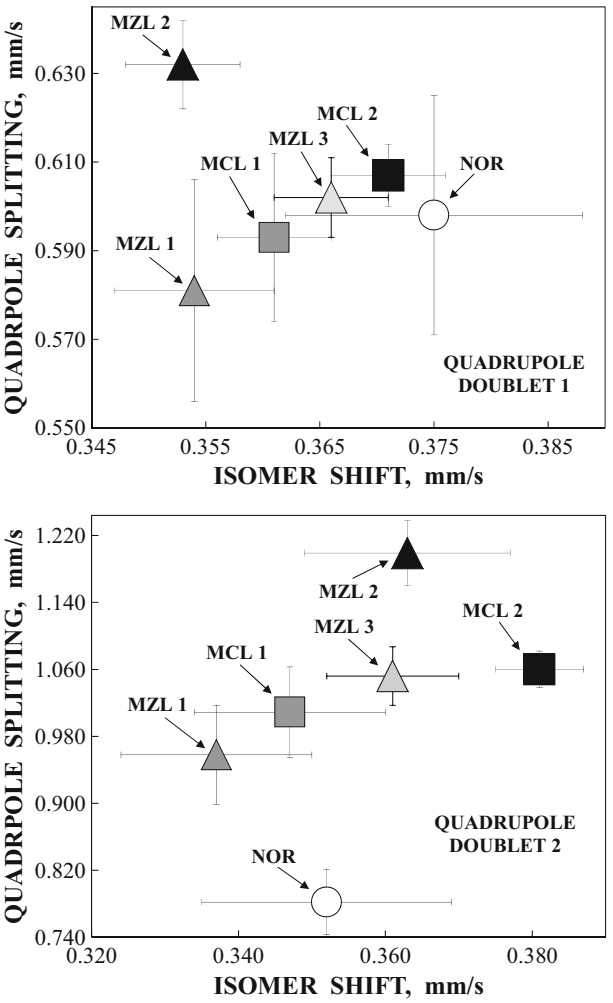

Fig. 3 Small differences in Mössbauer hyperfine parameters for quadrupole doublets 1 and 2 obtained using the simple heterogeneous iron core model: normal spleen (**NOR**) and spleen tissues from patients with mantle cell lymphoma (**MCL 1** and **MCL 2**) and marginal zone B-cell lymphoma (**MZL 1**, **MZL 2** and **MZL 3**)

samples are similar to each other. All samples contain at least paramagnetic (PM) and ferrimagnetic (FM) (probably magnetite Fe_3O_4 with $T_C = 853$ K) components embedded in a diamagnetic matrices. The PM phases are dominant at the low temperatures and their shape adhere closely to the Curie-Weiss (CW) law: (1) $\chi(T) = \chi_0 + C/(T–\Theta)$, where $\chi = M/H$, χ_0 is the temperature independent part, C is the Curie constant, and Θ is the CW temperature. The differences in their M(T) plots shape (ZFC and FC curves are shown in Fig. 5) stem from the change of the relative amount of the PM component. On the other hand all isothermal M (H) curves (measured at 5 or at 25 K and shown in Fig. 6) are quite similar to each other and can be fitted as: (2) $M(H) = M_S + \chi H$, where M_S is the spontaneous ferromagnetic

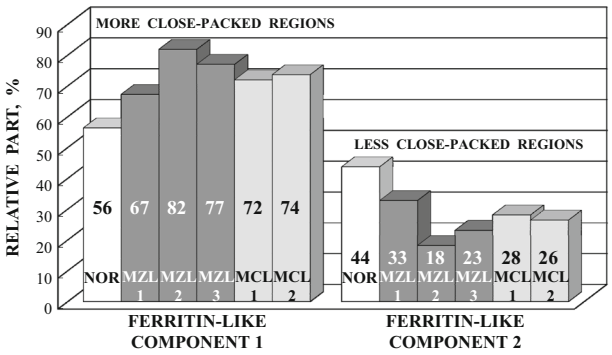

Fig. 4 Relative parts of quadrupole doublets 1 and 2 related to ferritin-like components with more and less close packed iron core regions: normal spleen (**NOR**) and spleen tissues from patients with mantle cell lymphoma (**MCL 1** and **MCL 2**) and marginal zone B-cell lymphoma (**MZL 1**, **MZL 2** and **MZL 3**)

(FM) magnetization and χH is the linear (PM and diamagnetic) intrinsic susceptibility. For the sake of clarity, we shall describe first the isothermal M(H) data (Fig. 6).

(i) In order to deduce the PM contribution, the M(H) curves for normal (NOR) and MCL 1 samples were measured at 25 K (see Fig. 6). In both cases the experimental branch first rises up to around 7–10 kOe and then turns to negative values with constant slopes. Using (2) we deduce the M_S values as 0.046(2) and 0.015(2) emu/g, respectively. Assuming magnetite (M_S = 96 emu/g) as the FM phase, these M_S values correspond to ∼470 or ∼156 ppm of Fe_3O_4, values which are below the detection limit of the Mössbauer spectroscopy technique (see below). For all the rest samples shown in Fig. 6, the M(H) curves were measured at 5 K where the PM components are dominant, thus all extracted χH plots are positive. All M_S values have the same order of magnitude as for the plots measured at 25 K, indicating a common origin. The minor differences of M_S stem from changes in the relative Fe_3O_4 concentration. Due to its high T_C (853 K) the M_S values at 5 and 25 K are almost identical.

(ii) As stated above, the M(T) plots are composed of two major components. The monotonic decrease with increasing temperatures in both ZFC and FC branches is due to the PM phase, whereas the high T_C of magnetite (a temperature currently inaccessible by our equipment) dictates that *at low applied fields* the two curves merge at RT (see Fig. 5, MZL 3). In addition, Fig. 5, NOR shows a broad pronounced peak at 45–65 K in the FC plot of the normal healthy spleen tissue. This peak is related to the spontaneous solidification of adsorbed oxygen on the sample surface [22]. The appearance of this broad peak in both ZFC and FC branches, depends on the handling process of the sample, e.g. on whether it was exposed for a long time to air. On the other hand, the sharp rise at Fig. 5, MCL 1 definitely points to the Verwey transition of magnetite. This transition refers to crystal lattice changes from a monoclinic structure to the cubic inverse spinel structure which persists at elevated temperatures [23]. The sharp peak in Fig. 5 for MCL 2 is not related to adsorbed oxygen since it does not show up in the FC branch. This peak is elusive and absent in FC branch. The peak's origin in the ZFC branch only is not clear yet. Note that in contrast to the case of human liver from

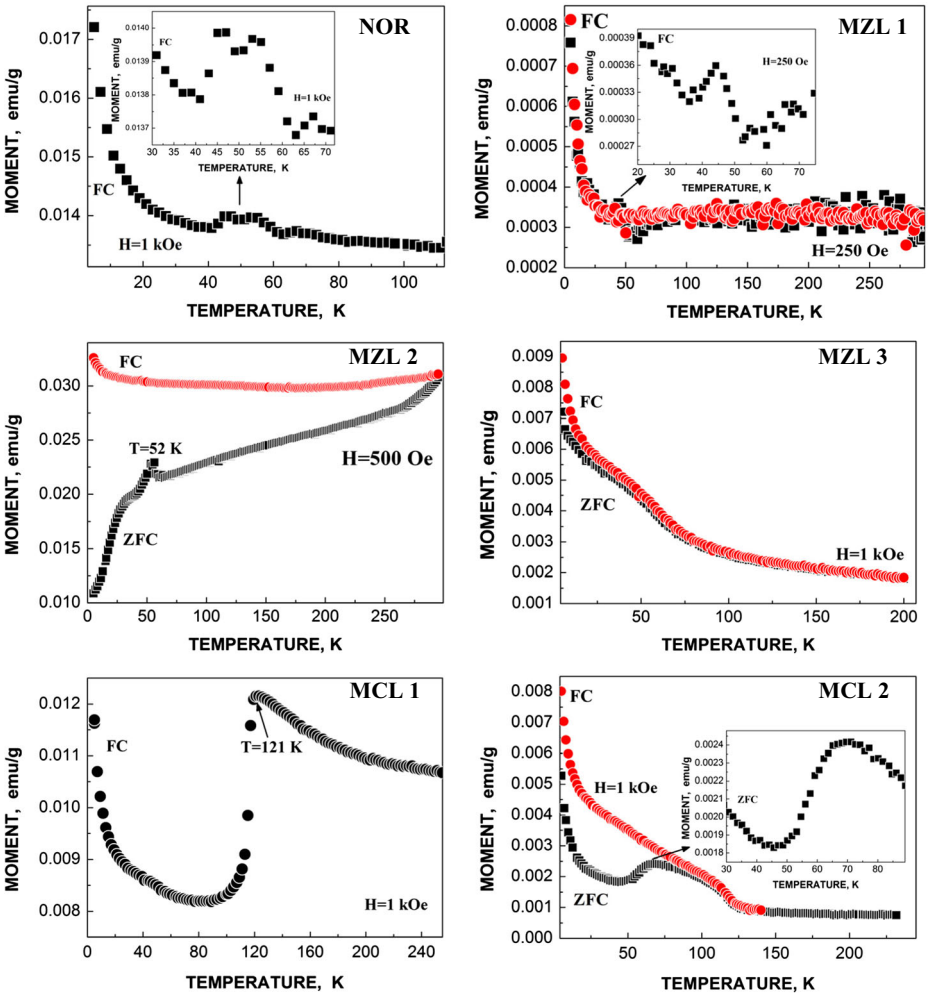

Fig. 5 ZFC and FC curves measured at 1 kOe for normal spleen tissue (**NOR**) and spleen tissues from patients with mantle cell lymphoma (**MCL 1** and **MCL 2**) and marginal zone B-cell lymphoma (**MZL 1**, **MZL 2** and **MZL 3**)

patient with acute myeloleukemia [24], as expected, the FC branch lies always above the ZFC one.

For MCL 2 and MZL 1 in Fig. 5, the two ZFC and FC curves are almost identical which may indicate the absence of magnetite. However their M(H) plots and the M_S values (Fig. 5, MCL 2 and MZL 1) which are very similar to all the rest curves may exclude this assumption. This observation needs some more extensive studies. The relative high $M_S = 0.82$ emu/g for MZL 2 (Fig. 6) indicates that the magnetite concentration in this tissue is about 2–3 times higher than for most of the samples studies. This implies a different M(T) behavior. Indeed the upraising at low temperature (Fig. 5, MZL 2) is obscured in both ZFC and FC branches which merge at RT as mentioned above. The tiny peak at 52 K due to oxygen in the ZFC plot is barely observed in the higher FC branch.

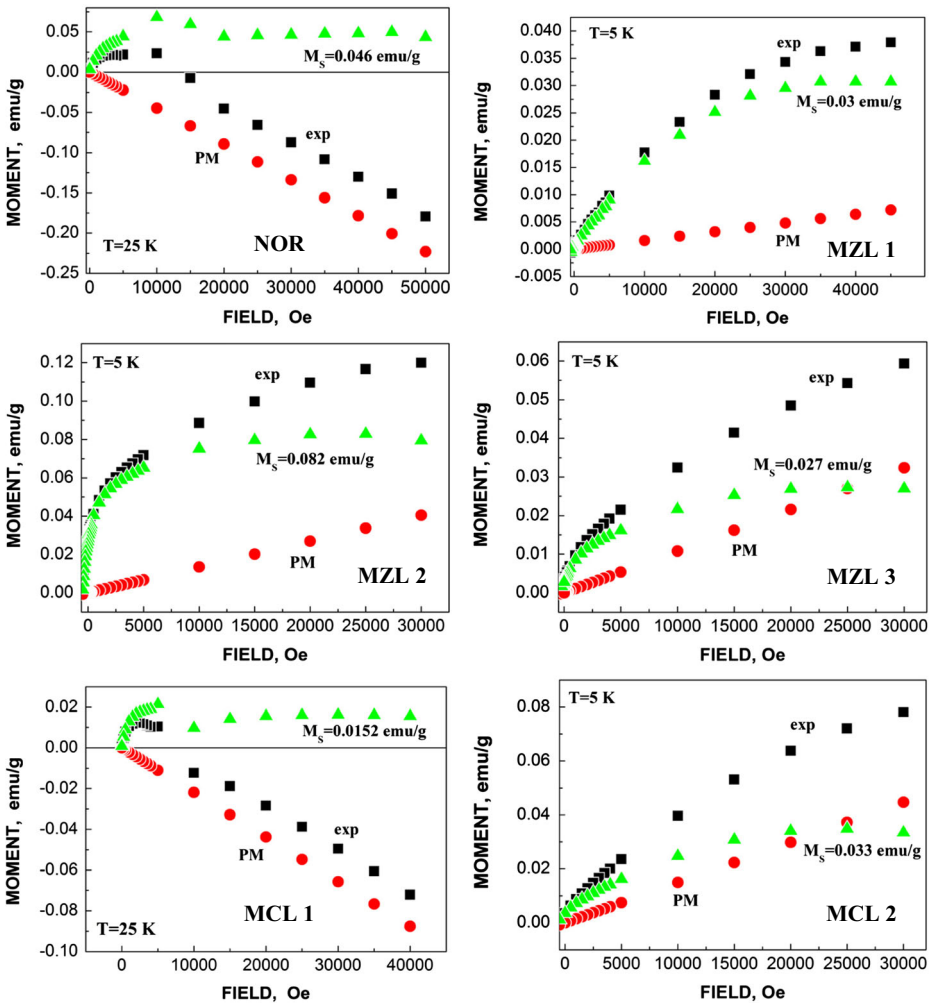

Fig. 6 Isothermal magnetization curves for normal spleen tissue (**NOR**) and spleen tissues from patients with mantle cell lymphoma (**MCL 1** and **MCL 2**) and marginal zone B-cell lymphoma (**MZL 1**, **MZL 2** and **MZL 3**); **exp** is experimental branches, **PM** is a paramagnetic contribution, $\mathbf{M_S}$ is the saturation moment, **T** is a temperature

4 Conclusions

Magnetization measurements performed at 5 K demonstrated small differences in the saturation magnetic moments (in emu/g) which were: ∼0.046 (NOR), ∼0.015 (MCL 1), ∼0.033 (MCL 2), ∼0.03 (MZL 1), ∼0.082 (MZL 2), and ∼0.027 (MZL 3), and the presence of paramagnetic components and tiny amount of magnetite. Mössbauer spectra of spleen tissues can be fitted well using two quadrupole doublets related to the ferritin-like iron (within the simple heterogeneous iron core model) and to the residual methemoglobin with different content. The relative ferritin-like iron content appeared to be different in the studied samples. Mössbauer hyperfine parameters demonstrated small variations for healthy and

patients' spleen tissues for both ferritin-like components 1 and 2 in the spectra. On the basis of the simple heterogeneous iron core model the differences in the relative parts of more or less close packed FeOOH core regions in ferritin molecules were revealed for healthy human spleen tissue and spleen tissues from patients with MCL and MZL. These results demonstrate that the iron-core structure in ferritin molecules in spleen may be changed as a result of the slightly modified process of iron accumulation in ferritin in case of the studied hematological malignancies.

Acknowledgements This work was supported by the Ministry of Education and Science of the Russian Federation (the Project # 3.1959.2017/4.6) and the Act 211 Government of the Russian Federation, contract No. 02.A03.21.0006.

References

1. Theil, E.C.: Ann. Rev. Biochem. **56**, 289–315 (1987)
2. Brooks, R.A., Vymazal, J., Goldfarb, R.B., Bulte, J.W., Aisen, P.: Mag. Res. Med. **40**, 227 (1998)
3. Pan, Y.-H., Sader, K., Powell, J., Bleloch, A., Gass, M., Trinick, J., Warley, A., Li, A., Brydson, R., Brown, A.: J. Struct. Biol. **166**, 22–31 (2009)
4. Galvez, N., Fernandez, B., Sanchez, P., Cuesta, R., Ceolin, M., Clemente-Leon, M., Trasobares, S., Lopez-Haro, M., Calvino, J.J., Stephan, O., Dominguez-Vera, J.M.: J. Am. Chem. Soc. **130**, 8062–8068 (2008)
5. Martínez-Pérez, M.J., Miguel, R., Carbonera, C., Martínez-Júlvez, M., Lostao, A., Piquer, C., Gómez-Moreno, C., Bartolomé, J., Luis, F.: Nanotechnology **21**, 465707 (2010)
6. Oshtrakh, M.I., Alenkina, I.V., Klencsár, Z., Kuzmann, E., Semionkin, V.A.: Spectrochim. Acta A Mol. Biomol. Spectrosc. **172**, 14–24 (2017)
7. Papaefthymiou, G.C.: Biochim. Biophys. Acta **1800**, 886–897 (2010)
8. Kamnev, A.A., Kovács, K., Alenkina, I.V., Oshtrakh, M.I.: In: Sharma V.K., Klingelhofer G., Nishida T. (eds.) Mössbauer Spectroscopy: Applications in Chemistry, Biology and Nanotechnology, 1st edn, pp. 272–291. Wiley (2013)
9. Kamnev, A.A., Tugarova, A.V.: Talanta **174**, 819–837 (2017)
10. Oshtrakh, M.I., Semionkin, V.A.: Spectrochim. Acta A Mol. Biomol. Spectrosc. **100**, 78–87 (2013)
11. Oshtrakh, M.I., Semionkin, V.A.: AIP Conference Proceedings, vol. 1781, 020019. AIP Publishing, Melville (2016)
12. Oshtrakh, M.I., Semionkin, V.A., Milder, O.B., Novikov, E.G.: J. Mol. Struct. **924–926**, 20–26 (2009)
13. Oshtrakh, M.I., Alenkina, I.V., Milder, O.B., Semionkin, V.A.: Spectrochim. Acta A Mol. Biomol. Spectrosc. **79**, 777–783 (2011)
14. Oshtrakh, M.I., Alenkina, I.V., Vinogradov, A.V., Kumar, A., Berkovsky, A.L., Zakharova, A.P., Konstantinova, T.S., Novikov, E.G., Semionkin, V.A.: J. Radioanal. Nucl. Chem. **309**, 317–332 (2016)
15. Oshtrakh, M.I., Alenkina, I.V., Vinogradov, A.V., Konstantinova, T.S., Kuzmann, E., Semionkin, V.A.: Biometals **26**, 229–239 (2013)
16. Oshtrakh, M.I., Alenkina, I.V., Vinogradov, A.V., Konstantinova, T.S., Semionkin, V.A.: Hyperfine Interact. **222**, 55–60 (2013)
17. Oshtrakh, M.I., Alenkina, I.V., Vinogradov, A.V., Konstantinova, T.S., Semionkin, V.A.: Hyperfine Interact. **231**, 123–130 (2015)
18. Alenkina, I.V., Oshtrakh, M.I., Felner, I., Vinogradov, A.V., Konstantinova, T.S., Semionkin, V.A.: AIP Conference Proceedings, vol. 1781, 020010. AIP Publishing, Melville (2016)
19. Oshtrakh, M.I., Semionkin, V.A., Milder, O.B., Novikov, E.G.: J. Radioanal. Nucl. Chem. **281**, 63–67 (2009)
20. Semionkin, V.A., Oshtrakh, M.I., Milder, O.B., Novikov, E.G.: Bull. Rus. Acad. Sci.: Phys. **74**, 416–420 (2010)
21. Oshtrakh, M.I., Alenkina, I.V., Semionkin, V.A.: Hyperfine Interact. **237**, 145 (2016)
22. Bandow, S., Yamaguchi, T., Iijima, S.: Chem. Phys. Lett. **401**, 380–384 (2005)
23. Kosterov, A.: In: Gubbins D., Herrero-Bervera E. (eds.) Encyclopedia of Geomagnetism and Paleomagnetism, pp. 515–525. Springer, Dordrecht (2007)
24. Felner, I., Alenkina, I.V., Vinogradov, A.V., Oshtrakh, M.I.: J. Mag. Mag. Mat. **399**, 118–122 (2016)